

Effect of Domain Size and Grid Spacing on Flow Past A Circular Cylinder At Low Reynolds Number

Nidhul K

Assistant Professor

Dept. of Mechanical Engg.

Royal college of Engineering and Technology Govt.
Thrissur, India

Sunil A S

Associate Professor

Dept. of Mechanical Engg.

Engineering College Thrissur
Thrissur, India

Benphil C M

Assistant Professor

Dept. of Mechanical Engg.

College of Engineering Adoor
Pathanamthitta, Thrissur

Abstract— In this paper, the effect of size of rectangular flow domain and grid spacing on flow past a circular cylinder at low Reynolds number is numerically investigated using ANSYS Fluent. Two dimensional steady incompressible flow past a circular cylinder is solved numerically using finite volume method with second order accuracy in space. Pressure-velocity coupling scheme employed is SIMPLEC. A domain independent study was conducted by varying the size of flow domain to ensure that the simulation results were independent of domain size. Then on the flow domain chosen, grid independence study is conducted so as to optimize computational hardware resource and time while ensuring that the results predicted are accurate. The flow pattern and flow characteristics past a circular cylinder at low Reynolds number were studied by means of vorticity magnitude contour, flow streamlines, coefficient of drag and variation of x-component of velocity.

Keywords — grid; circular cylinder; Reynolds number; incompressible flow; coefficient of drag, coefficient of pressure

I. INTRODUCTION

Vortex shedding behind bluff bodies is of concern for many engineering applications. Bluff bodies are structures with shapes that significantly disturb the flow around them, as opposed to flow around a streamlined body. A bluff body is one in which the length in the flow direction is close to or equal to the length perpendicular to the flow direction. Examples of bluff bodies include circular cylinders, square cylinders and rectangular cylinders. Flow around a circular cylinder is a fundamental fluid mechanics problem of practical importance such as in submarines, off shore structures, bridge piers, pipelines etc. The laminar steady viscous flow behind a circular cylinder has been the subject of numerous experimental and numerical studies.

Zakir Faruquee et.al [1] conducted domain independent study for flow past circular cylinder using circular domain whose far-field boundary radius was varied from 10D-60D. In all cases, the same cell distribution was used for common subdomains. The influence of the far-field boundary on the drag coefficient was studied. Behr et al. [2] studied the influence of the location of the lateral boundaries on the unsteady flow past a circular cylinder at $Re = 100$. They have suggested that the lateral boundaries should be away from the cylinder by a distance of at least 8 cylinder diameters. Inoue et.al [3] constructed a non-uniform mesh but divided the computational domain into three regions, each with a different

grid ratio. Mohamed Sukri Mat Ali et.al [4] numerically investigated the sensitivity of the computed flow field to flow parameters for a flow with Reynolds number 150. They constructed computational meshes based on reasonable estimates of cell size and grid stretching ratios. Sumer et.al [5] investigated and reported that the flow field over the circular cylinder is symmetric at low values of Reynolds number. As the Reynolds number increases, flow begins to separate behind the cylinder causing vortex shedding which is an unsteady phenomenon. Kovaszny [6] and Roshko [7] determined experimentally that for Re less than 40, the flow remains laminar, two-dimensional and steady, but can become unstable under the influence of external excitation. Braza et.al [8] showed that when the Reynolds number is increased beyond 40, not every destabilization of the flow, random or not, can be damped out.

II. NUMERICAL SIMULATION PROCEDURE

A. Governing equations

A single circular cylinder subjected to a uniform upstream air flow in an open atmosphere is the physical model of the problem. Flow over the cylinder is governed by the partial differential equations derived from the laws of conservation of mass (continuity equation) and momentum (Navier–Stokes equations), which can be written as follows:

$$\frac{\partial \rho}{\partial t} + \text{div}(\rho V) = 0 \quad (1)$$

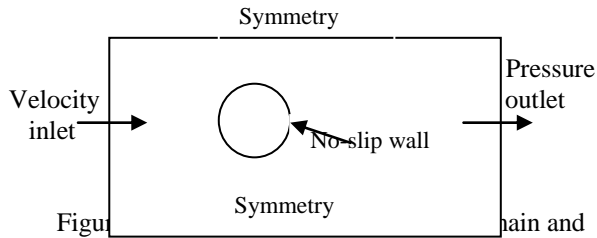
$$\frac{\partial}{\partial t}(\rho u) + \text{div}(\rho V u) = -\frac{\partial p}{\partial x} + \text{div}(\mu \text{grad} u) + B_x \quad (2)$$

$$\frac{\partial}{\partial t}(\rho v) + \text{div}(\rho V v) = -\frac{\partial p}{\partial y} + \text{div}(\mu \text{grad} v) + B_y \quad (3)$$

Where ρ is the fluid density, μ is the fluid viscosity, V is the velocity vector of the flow field, p is the pressure, and u and v are the velocity components in the x - and y -directions, respectively. B_x and B_y are also the body forces per unit volume, which are negligible in the present study. The fluid is assumed to be incompressible, and its properties has been taken as $\rho=1.225 \text{ kg/m}^3$ and $\mu=1.7894 \times 10^{-5} \text{ kg/m s}$.

B. Computational domain

The governing equations (1)–(3) have been applied in the computational domain (Fig.1) of the physical model. A rectangular domain is employed in this study. To minimize the effect of the far-field boundary conditions, the outer boundary of the computational domain must be placed sufficiently far away from the cylinder.



A computational domain extending up to a length of 4D (i.e., 4 times cylinder diameter) in the upstream, to a length of 4D in transverse directions and 9D in the downstream direction from the center of the cylinder was initially employed. Then, to determine an appropriate location for the outer boundaries, length of boundaries was varied upto 16D in upstream and transverse direction and 21D in downstream direction. In all cases, the same cell distribution was used for common subdomains. The influence of the far-field boundaries on the drag coefficient is given in Table 1 at $Re = 40$.

TABLE 1

Effect of far-field boundaries on the drag coefficient for a circular cylinder at $Re = 40$

Far-field boundaries	No. of cells	C_D
4D, 4D and 9D	33120	1.89
5D, 5D and 10D	40392	1.79
6D, 6D and 11D	49704	1.72
7D, 7D and 12D	60480	1.68
8D, 8D and 13D	74200	1.65
9D, 9D and 14D	91104	1.63
10D, 10D and 15D	110424	1.61
11D, 11D and 16D	134140	1.60
12D, 12D and 17D	162960	1.59
13D, 13D and 18D	197274	1.58
14D, 14D and 19D	240640	1.57
15D, 15D and 20D	291588	1.56
16D, 16D and 21D	353918	1.56

As seen from this table, moving the outer boundaries from 15D, 15D and 20D, does not have any noticeable effect on the flow parameter. Therefore, computational domain having an upstream length of 15D, transverse length of 15D and downstream length of 20D was chosen to simulate the unbounded flow past circular cylinder.

The application of appropriate boundary conditions at the cylinder surface and at the outer boundary is crucial for accurate simulation. A uniform approach velocity was imposed on the upstream of the outer boundary of the computational domain, while symmetry condition was imposed on top and bottom free-streams and a pressure outlet condition was imposed on the downstream. No-slip condition was applied along the cylinder wall. In this study, the QUICK method of interpolation was used for solving velocity and momentum. The SIMPLER method was employed for the pressure– velocity coupling for all simulations. The second order interpolation scheme was applied for pressure. Convergence criterion employed is 10^{-6} .

III. GRID INFLUENCE

Within the scope of predicting the flow field around a square cylinder using numerical analysis, many similar investigations have been made, but the results always show small discrepancies even though the overall global trends are similar. One of the reasons for these discrepancies is the difference in the construction of the mesh. Generally, the accuracy of a numerical solution increases as the number of cells increases. But employing a larger number of cells requires more computer hardware resource and computing time. All simulations performed in this study employed quadrilateral cells. Grid spacing was gradually increased from the cylinder surface towards the outer boundaries in order to avoid sudden distortion and skewness, and to provide a sufficiently clustered mesh near the cylinder wall where the flow gradients are large and to capture flow regime within the boundary layer.

Grid independency was achieved in this study according to the procedure outlined by Yunus A. cengel and Michael A. Boles [10]. Several meshes, with increasing refinement, were tested to ensure that the solution was independent of the mesh. These meshes and the drag coefficient (C_D) predictions are reported in Table 2 for the case of a circular cylinder at $Re = 40$. It is observed that initially with 27300 cells, the value of coefficient of drag is overpredicted. Whereas the value does not vary for mesh finer than 81952 cells.

TABLE 2

Effects of cell density on drag coefficient for a circular cylinder at $Re = 40$

No. of cells	C_D
27300	1.560
39312	1.562
56560	1.563
81952	1.564
116392	1.564

IV. RESULTS AND DISCUSSIONS

From the domain independence study, it was observed that rectangular domain with dimensions $15D$ in upstream direction, $15D$ in transverse direction and $20D$ in the downstream direction predicts the results accurately for flow past a circular cylinder at $Re=40$. Then grid independence study was conducted on this domain with grid refinement starting from 27300 cells. It was observed that grid refinement beyond 81952 cells did not make any significant changes on flow parameters. Variation in the value of drag coefficient was taken for grid refinement study.

2D steady and incompressible flow over a circular cylinder was simulated at $Re=40$ using the above mentioned computational domain and grid. Flow at $Re=40$ is laminar and steady. As flow approaches the leading point of a circular cylinder, the fluid is brought to rest, causing a pressure rise and a boundary layer develops along the surface. The leading point is called the forward stagnation point. For very low Reynolds number ($Re < 5$), the flow splits into two symmetrically equal parts and passes around the cylinder to the rear stagnation point. When Reynolds number is increased, small size eddies develop in the immediate vicinity of the rear stagnation point of the cylinder, where the velocity is extremely small and pressure gradient is unfavorable. The recirculation zone remains steady, two dimensional and symmetrical about the streamwise center line of the flow. The contours of vorticity magnitude at $Re=5$ and $Re=40$ are shown in fig.2.

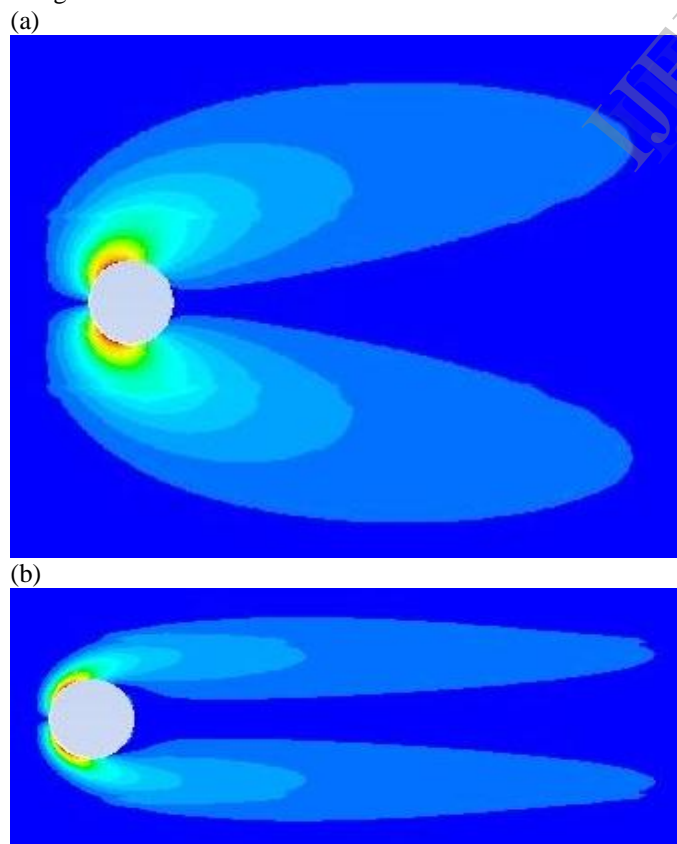


Figure 2: Contours of vorticity magnitude
(a) At $Re=5$ and (b) At $Re=40$

The flow streamlines for flow past circular cylinder at $Re=5$ and $Re=40$ are shown in fig.3. At $Re=40$, only recirculation eddies are formed immediately downstream of the cylinder, near the rear stagnation point as indicated by streamlines.

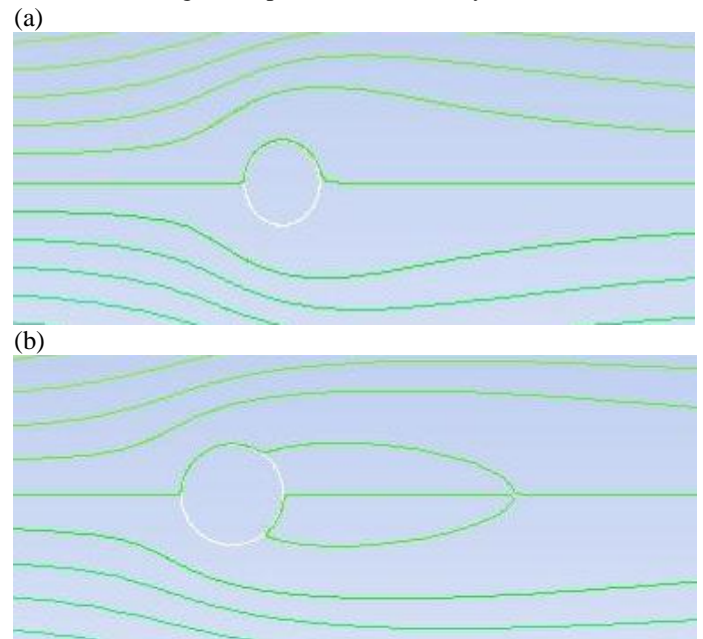


Figure 3: Flow streamlines
(a) At $Re=5$ and (b) At $Re=40$

Variation of x-component along the wake centerline is shown by non-dimensionalised parameter of x-component velocity. Fig.4 shows the variation of x-component velocity along wake centerline at $Re=5$ and $Re=40$.

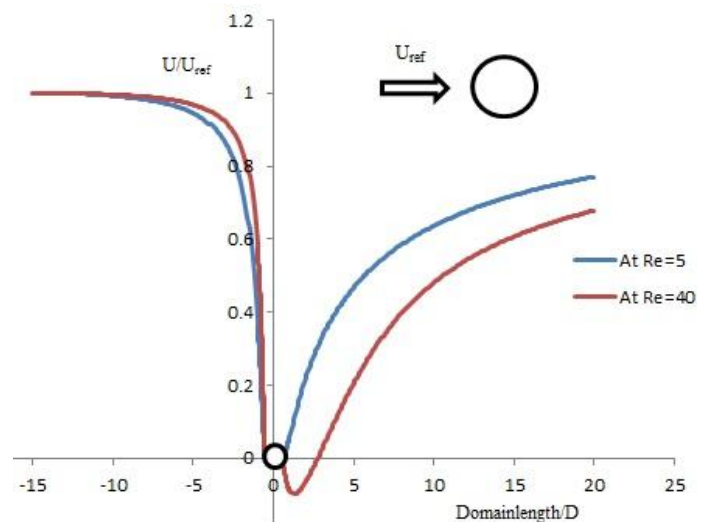


Figure 3: U/U_{ref} along the wake centerline

REFERENCES

- [1] Zakir Faruquee, David S-K. Ting, Amir Fartaj, Ronald M. Barron and Rupp Cariveau, "The effects of axis ratio on laminar fluid flow around an elliptical cylinder," *International Journal of Heat and Fluid Flow* 28 (2007) 1178–1189.
- [2] Behr, M., Hastreiter, D., Mittal, S., Tezduyar, T.E., "flow past a circular cylinder: dependence of the computed flow field on the location of the lateral boundaries", *Comput. Methods Appl. Mech. Eng.*(1995) 123, 309–316.
- [3] Inoue, Iwakam and Hatakeyama, "Aeolian tones radiated from flow past two square cylinders in a side-by-side arrangement." *Physics of Fluids*,(2006) 18(4), 046104.
- [4] Ali, M.S.M., Doolan, C.J., Wheatley, V., "Grid convergence study for a two dimensional simulation of flow around a square cylinder at a low Reynolds number", In: *Seventh International Conference on CFD in The Minerals and Process Industries.*(2009) CSIRO, Melbourne, Australia.
- [5] D. Sumner, J. L. Heseltine and O. J. P. Dansereau, "Wake structure of a finite circular cylinder of small aspect ratio", *Experiments in Fluids*, November 2004, Volume 37, Issue 5, pp 720-730.
- [6] Kovasznay, L.S.G., "Hot-wire investigation of the wake behind cylinders at low Reynolds number", *Proc. Roy. Soc. A* (1949) 198, 174.190.
- [7] Roshko, A., "On the development of turbulent wakes from vortex streets." *National Advisory Committee for Aeronautics*,(1954) Report 1191.
- [8] Braza, M., Chassaing, P. and Ha Minh, H., "Numerical study and physical analysis of the pressure and velocity fields in the near wake of a circular cylinder." *J. Fluid Mech.*(1986) 165, 79–130.
- [9] Okajima, A., "Numerical analysis of the flow around an oscillating cylinder", In P.W. Bearman (Ed.), *Proc. 6th Int. Conf. Flow-Induced Vibration*, London, UK,(1995) 10-12 April, pp. 1–7. Balkema, Rotterdam.
- [10] Yunus A. Cengel & Michael A. Boles, "Fluid Mechanics: Fundamentals and Applications", Published by McGraw-Hill.

IJERT